



## UvA-DARE (Digital Academic Repository)

### The stress-axis in multiple sclerosis: Clinical, cellular and molecular aspects

Melief, J.

**Publication date**  
2014

[Link to publication](#)

#### **Citation for published version (APA):**

Melief, J. (2014). *The stress-axis in multiple sclerosis: Clinical, cellular and molecular aspects*. [Thesis, fully internal, Universiteit van Amsterdam]. Boxpress.

#### **General rights**

It is not permitted to download or to forward/distribute the text or part of it without the consent of the author(s) and/or copyright holder(s), other than for strictly personal, individual use, unless the work is under an open content license (like Creative Commons).

#### **Disclaimer/Complaints regulations**

If you believe that digital publication of certain material infringes any of your rights or (privacy) interests, please let the Library know, stating your reasons. In case of a legitimate complaint, the Library will make the material inaccessible and/or remove it from the website. Please Ask the Library: <https://uba.uva.nl/en/contact>, or a letter to: Library of the University of Amsterdam, Secretariat, Singel 425, 1012 WP Amsterdam, The Netherlands. You will be contacted as soon as possible.

# [4]

---

## **Phenotyping primary human microglia: tight regulation of LPS responsiveness**

Jeroen Melief, Nathalie Koning, Karianne Schuurman, Martijn van de Garde, Joost Smolders, Robert Hoek, Marco van Eijk, Jörg Hamann, and Inge Huitinga

---

## ABSTRACT

Much is still unknown about mechanisms underlying the phenotypical and functional versatility of human microglia. Therefore, we developed a rapid procedure to isolate pure microglia from post-mortem human brain tissue and studied their immediate *ex vivo* phenotype and responses to key inflammatory mediators. Microglia were isolated, along with macrophages from the choroid plexus by tissue dissociation, density gradient separation and selection with magnetic microbeads. By flow cytometry, microglia were identified by a CD11b<sup>+</sup>CD45<sup>dim</sup> phenotype and a smaller size compared to CD11b<sup>+</sup>CD45<sup>high</sup> macrophages. Interestingly, white matter microglia from donors with peripheral inflammation displayed elevated CD45 levels and increased size and granularity, but were still distinct from macrophages. The phenotype of isolated microglia was further specified by absent surface expression of CD14, CD200 receptor and mannose receptor (MR, CD206), all of which were markedly expressed by macrophages. Microglia stimulated immediately after isolation with LPS and IFN $\gamma$  failed to upregulate TNF $\alpha$  or CCR7. Notably, responsiveness to LPS and IFN $\gamma$  was clearly instigated in microglia after overnight preculture, which coincided with a strong upregulation of CD14. Culture of microglia with IL-4 resulted in the induction of HLA-DR and CCL18 but not MR, whereas culture with dexamethasone did induce MR, in addition to CD163 and CCL18. In conclusion, this study demonstrates phenotypic changes of microglia associated with peripheral inflammation, and reveals tight regulation of responses to LPS and IFN $\gamma$  as well as distinct microglial responses to IL-4 and glucocorticoids. These findings are of high relevance to studies on human microglia functioning in health and disease.

## INTRODUCTION

As the key immunocompetent cells of the central nervous system (CNS), microglia play a crucial role in both innate and adaptive immune responses in the brain.<sup>102,103,105</sup> Microglia are cells of the myeloid lineage that are morphologically characterized by a small soma with extensive radial ramifications, which they use to actively survey the microenvironment under physiological conditions.<sup>107</sup> Upon activation, microglia may proliferate and, through several transitional stages, adopt an amoeboid, macrophage-like morphology.<sup>108,109</sup> In their function as surveyor of parenchymal brain homeostasis, microglia are highly responsive to microenvironmental alterations due to local damage, inflammation or infection. Another well recognized feature of microglia is their sensitivity to inflammation outside the CNS.<sup>194</sup> Peripheral inflammatory conditions or systemic inflammation can alter microglia activation status or even lead to active and detrimental microglial immune responses, a phenomenon that is suggested to be involved in exacerbation of neurodegenerative disorders and delirium.<sup>110,111</sup>

Depending on their activation status and the encountered challenge, microglia are able to exert a variety of effector functions, which may be either neurotoxic or neuroprotective.<sup>112</sup> The functional versatility and either benign or detrimental role of microglia in neurodegeneration and inflammation has led to a strong interest in the mechanisms underlying their phenotypic switches. One of the main questions of interest is to what extent microglia exhibit features of classical (M1) and alternative (M2) macrophage activation. M1 activation refers to pro-inflammatory immune responses of macrophages induced by lipopolysaccharide (LPS) or interferon-gamma (IFN- $\gamma$ ), alone or in combination, and leads to production of various effector molecules that are known to confer neurotoxicity, such as tumor necrosis factor alpha (TNF $\alpha$ ), interleukin-6 (IL-6) and reactive oxygen species (ROS). Conversely, M2 activation comprises the induction of various tissue repair and immunoregulatory pathways through macrophages by compounds such as IL-4 (M2a activation) and glucocorticoids (M2c activation) and is associated with expression of inflammatory mediators that suppress inflammation and promote neuroprotection, such as IL-10

and transforming growth factor-beta (TGF- $\beta$ ).<sup>81–84,195</sup> In this respect, a procedure for rapid isolation of microglia from post-mortem human brain tissue would be a highly valuable tool. Not only would it enable studies on microglial immune responses immediately after isolation, but it would also allow for *in vitro* assays on various effector functions and facilitate transcriptomic and proteomic analyses.

In 1997, Sedgwick and co-workers described the isolation and flow cytometric analysis of human microglia from brain biopsies that originated from HIV-positive patients and other subjects.<sup>196</sup> Due to the lack of distinctive microglial cell surface markers, this study identified microglia by their CD11b<sup>+</sup>CD45<sup>dim</sup> phenotype to distinguish them from CD11b<sup>+</sup>CD45<sup>high</sup> monocytes from blood. However, this distinction may be distorted by upregulation of CD45 during microglia activation, which is well described in both human and rodent brain.<sup>197–199</sup> Taking this into account, our first aim was to establish whether CD11b and CD45 expression could be used to phenotypically differentiate microglia from peripheral macrophages in various inflammatory conditions. Next, we used magnetic cell sorting using CD11b expression in combination with flow cytometry to characterize the cell surface phenotype of primary microglia. To further study mechanisms involved in phenotypic as well as functional switches of microglia, our final objective was to establish whether they would show *in vitro* responses to M1 and M2 stimuli that are similar to those described for monocyte-derived macrophages (MDMs).

## MATERIALS & METHODS

### Donors and tissue

Donor tissue (table 1) was provided by the Netherlands Brain Bank. Informed consent was obtained for brain autopsy and the use of tissue and clinical information for research purposes. At autopsy, white matter (WM) from corpus callosum, grey matter (GM) from occipital cortex as well as choroid plexus was dissected and stored in Hibernate A medium (Brain Bits LLC, Springfield, IL, USA) at 4°C. The mean age was 78.4 y (range 49 – 98 y) and the mean post-mortem delay was 7:01 h (range

3:35-18:30 h). The average pH value of cerebrospinal fluid was 6.7 (range 6.0 – 7.2). Donors included did not have a neurological or psychiatric disorder, except for donor 8 and 16, who had Parkinson's disease (PD). These were included as they had no dementia and PD does not affect the corpus callosum and occipital cortex. Three donors had peripheral inflammatory conditions that are known to coincide with peripheral or even central elevations of pro-inflammatory cytokines: donor 3 (end-stage chronic obstructive pulmonary disease, COPD), donor 9 (sepsis) and donor 11 (severe chronic wound infection).<sup>200-203</sup> Cells from donors with either PD or peripheral inflammation were used for flow cytometric analysis and not for *in vitro* experiments.

## Isolation procedure

### *Tissue dissociation*

Isolation procedures were started within 2 to 24 h after autopsy. In total 3 to 6 g of WM or GM brain tissue and 0.3 to 1.2 g choroid plexus were meshed through a stainless steel sieve in a glucose-potassium-sodium buffer (GKN-BSA; 8 g/l NaCl, 0.4 g/l KCl, 1.77 g/l Na<sub>2</sub>HPO<sub>4</sub>·2H<sub>2</sub>O, 0.69 g/l NaH<sub>2</sub>PO<sub>4</sub>·H<sub>2</sub>O, 2 g/l D-(+)-glucose, pH 7.4) with 0.3% bovine serum albumin (Roche Diagnostics GmbH, Mannheim, Germany). All subsequent wash steps were performed with this GKN-BSA buffer, unless stated otherwise.

Enzymatic dissociation was done in 50 ml tubes (Greiner Bio-One GmbH, Frickenhausen, Germany). Based on weighing prior to mechanical dissociation, each tube contained 1 to 1.5 g of brain tissue, or choroid plexus. Dissociated brain tissue and choroid plexus were washed and centrifuged for 7 min at 1400 rpm and 4°C. Pellets were resuspended in 4 ml enzyme buffer (4 g/l MgCl<sub>2</sub>, 2.55 g/l CaCl<sub>2</sub>, 3.73 g/l KCl and 8.95 g/l NaCl, pH 6-7), followed by enzymatic digestion in 300 units/ml collagenase type I (Worthington, Lakewood, NJ, USA) and 200 mg/ml DNase I (Roche Diagnostics GmbH) for 1 h at 37°C while shaking.

*Density gradient separation*

After enzymatic dissociation, cells were washed and incubated for 2 min on ice in 10 ml cold erythrocyte lysis buffer (8.26 g/l  $\text{NH}_4\text{Cl}$ , 1 g/l  $\text{KHCO}_3$  and 0.037 g/l EDTA, pH 7.35). Subsequently, cells were washed and resuspended in 20 ml Percoll (Amersham Biosciences, Piscataway, NJ, USA) of  $\rho=1.03$ , then underlain with 10 ml Percoll of  $\rho=1.095$ , overlain with 5 ml GKN-BSA buffer and centrifuged for 35 min at 2500 rpm and 4°C with slow acceleration and no break. The myelin layer on top of the  $\rho=1.03$  Percoll phase was discarded. Cells were collected from the interface between  $\rho=1.095$  and  $\rho=1.03$  Percoll, washed, resuspended in GKN-BSA buffer and counted in a cell counting chamber using trypan blue. Next, cells were pooled per brain region and transferred to a polypropylene coated 12 ml tube (Greiner Bio-One) for further use.

*Magnetic-activated cell sorting*

Depletion of granulocytes and positive selection of microglia with respectively anti-CD15 and anti-CD11b conjugated magnetic microbeads (Miltenyi Biotec GmbH, Bergisch Gladbach, Germany) was done by magnetic-activated cell sorting (MACS) according to the manufacturer's protocol. Briefly, cells were incubated 8  $\mu\text{l}$  CD15 microbeads in a total volume of 100  $\mu\text{l}$  for 15 min at 4°C. After this, cells were washed, resuspended in 500  $\mu\text{l}$  beads buffer and transferred to an MS column placed in a magnetic field.

The flow-through, containing the unlabeled cells, was collected and washed. Cells were subsequently incubated with 15  $\mu\text{l}$  CD11b microbeads in a total volume of 100  $\mu\text{l}$  for 15 min at 4°C. After this, cells were washed and resuspended in 500  $\mu\text{l}$  beads buffer and transferred to an MS column placed in a magnetic field. The eluted cells were used for culture purposes and, along with the flow-through, evaluated for proper separation of microglia from other cell types by flow cytometry.

**Table 1** Overview of donors included in the study

Donor	NBB no.	Age	Sex	pH CSF	PMD	Death cause
1	2009-012	78	M	6.52	<17:20	Heart failure
2	2009-102	92	F	6.24	06:55	Cachexia and general deterioration
3	2010-007	85	F	7.07	05:19	End-stage COPD
4	2010-038	79	F	6.30	18:30	Heart failure
5	2010-058	98	M	6.54	05:50	Cachexia
6	2010-062	94	F	7.04	05:50	Cachexia
7	2010-070	60	F	6.80	07:30	Heart failure
8	2010-107*	61	M	6.72	05:00	Euthanasia
9	2010-115	70	M	7.20	03:35	Sepsis
10	2011-021	85	F	n.d.	07:05	Kidney failure
11	2011-028	81	F	6.67	04:25	Heart failure
12	2011-039	91	F	6.50	04:15	Heart failure
13	2011-044	51	M	7.05	07:45	Suicide
14	2011-046	89	F	6.76	04:45	Euthanasia
15	2011-049	83	F	6.04	04:40	Metastasized pancreas carcinoma
16	2011-066*	81	F	6.76	05:55	Sudden death e.c.i.
17	2011-069	49	M	6.23	06:15	Non-Hodgkin lymphoma
18	2011-070	87	F	6.72	06:59	Heart failure
19	2011-072	76	F	6.87	07:15	Heart failure
20	2011-081	55	M	6.88	07:30	Euthanasia
21	2011-090	85	F	6.51	08:25	Dehydration and cachexia
22	2011-091	76	M	6.31	06:45	Lung cancer
23	2011-105	95	F	6.44	05:50	Euthanasia
24	2011-114	81	F	6.77	05:30	Respiratory insufficiency

The first column depicts donor numbers referred to in article text. Euthanasia was according to Dutch law. NBB no.=Netherlands Brain Bank registration number; PMD=post-mortem delay, time (h) between dying and the end of the autopsy; M=male; F= female; n.d.= not determined; COPD=chronic obstructive pulmonary disease; E.c.i.=e causa incognita. \* Donor with Parkinson's disease

## Flow cytometry

### *Quantification of CD11b and CD45 expression*

Cells were stained immediately after Percoll gradient separation, using antibodies with the following specificities: anti-human CD11b (immunoglobulin (Ig)G1, clone ICRF44, labeled with PE; eBioscience, San Diego, CA, USA), CD45 (IgG1, clone HI30, labeled with FITC; Dako, Glostrup, Denmark) and CD15 (IgM, clone HI98, labeled with APC; Biolegend, San Diego, CA, USA). A mouse isotype control anti-

body (IgG1, clone P3, labeled with FITC or PE; eBioscience) was used to determine background staining. Briefly,  $1 \times 10^5$  cells in 100  $\mu$ l GKN-BSA containing 5% human pooled serum (HPS) were incubated with antibodies for 30 min on ice in a 5 ml polypropylene round-bottom tube (BD Biosciences, San Diego, CA, USA) to prevent adherence of myeloid cells. Subsequently, cells were washed in GKN-BSA by centrifuging for 6 min at 1400 rpm and resuspended in 100  $\mu$ l GKN-BSA. About 15 min prior to flow cytometry, 2.5  $\mu$ l of 7-amino-actinomycin D (7AAD; BD Biosciences) was added per sample. Flow cytometric analysis was performed with identical instrument settings on a FACSCalibur machine (BD Biosciences), which was calibrated at least once a week, enabling the use of the geometric fluorescence intensity (geoMFI) of CD45 and CD11b for accurate quantification and comparison between experiments. Data were analyzed using FlowJo software version 8.7.1 (Treestar Inc. Ashland, OR, USA).

### *Phenotyping*

Antibodies were of the IgG1 isotype, unless stated otherwise, and had the following specificities: anti-human CD32 (clone 3D3, labeled with PE), CD45 (clone 2D1, labeled with PerCP), CD80 (clone L307.4, labeled with PE), CD86 (clone 2311 (FUN-1), labeled with FITC), CD163 (clone GHI/61, labeled with PE), MR (CD206; clone 19.2, labeled with APC; all from BD Biosciences); CD16 (clone LNK16, labeled with AF647), CD200R (clone OX108, labeled with AF647; both AbD Serotec, Oxford, UK), CD64 (clone 10.1, labeled with AF488), HLA-DR (IgG2a, clone L243, labeled with AF488; both Biolegend), CD14 (clone 61D3, labeled with PerCP-Cy5.5; eBioscience). Mouse isotype control antibodies (IgG1, clone MOPC-21, labeled with PerCP-Cy5.5, PE or APC; BD Biosciences; IgG2a, clone MOPC-173, labeled with AF488; Biolegend) were used to determine background staining. Cells were also stained with CD11b-, CD45- and CD15-specific antibodies used for FACSCalibur experiments, as described above. Flow cytometric analysis was performed on a FACSCanto machine (BD Biosciences) and the FlowJo software package (Treestar).

## Cell culture and stimulation

### *Primary human microglia*

In a 96-wells plate (Greiner Bio-One),  $1.0 \times 10^5$  MACS-isolated microglia were cultured in a total volume of 200  $\mu$ l Rosswell Park Memorial Institute medium (RPMI) with 10% heat-inactivated HPS per well for either 4 h or 18 h with 100 ng/ml LPS (*Salmonella minnesota* R595; Alexis Biochemicals, Lausen, Switzerland) alone, or in combination with IFN $\gamma$  (10 ng/ml; both from Peprotech, London, UK) or for 72 h with 40 ng/ml IL-4 (Peprotech) or 2 nM dexamethasone (Sigma Aldrich, Zwijndrecht, The Netherlands). Cells were harvested, after being checked for viability by microscopy, in 800  $\mu$ l Trizol reagent (Invitrogen, Carlsbad, CA, USA) and stored at -80°C for later use.

### *Monocyte-derived macrophages*

Peripheral blood mononuclear cells (PBMCs) were isolated by density gradient separation using Lymphoprep (Nycomed, Roskilde, Denmark) followed by isolation of monocytes using layers of 34%, 45% and 60% Percoll. Monocytes were taken from the 34–45% interface, washed in PBS and adhered to cell culture plastic for 1 h by 37°C. Non-adhering cells were removed, and further maturation towards macrophages was achieved by continued adherence to plastic in 12-well culture plates (Corning Incorporated, New York, NY, USA) in RPMI 1640 (BioWhittaker, Verviers, Belgium) and 10% HPS (BioWhittaker). MDMs were stimulated and analyzed like microglia.

## RNA isolation and cDNA synthesis

RNA isolation was performed as described previously, with minor adaptations.<sup>132</sup> After addition of 160  $\mu$ l chloroform (Sigma) to 800  $\mu$ l Trizol with cell lysates, samples were vortexed for 15 sec, allowed to rest at room temperature (RT) for 3 min and centrifuged for 15 min at 12,000 x g. The aqueous (top) phase was transferred to a new tube, after which an equal volume of 70% ethanol was slowly added. The mixture was then transferred to an RNeasy Mini column (Qiagen, Hilden, Germany). The RNA isolation was further done according to manufacturer's instructions. Con-

centration of extracted RNA was determined using a nanodrop (ND-1000; NanoDrop Technologies, Rockland, DE, USA). RNA integrity was assessed using a Bioanalyzer (2100; Agilent Technologies, Palo Alto, CA).

Synthesis of cDNA was done using the Quantitect Reverse Transcription Kit (Qiagen, Hilden, Germany) according to the manufacturer's protocol. For all samples, equal RNA inputs were used in a total volume of 12  $\mu$ l RNase free water. After addition of 2  $\mu$ l gDNA Wipeout Buffer (7x), samples were incubated at 42°C for 2 min. After addition of the master mix with RT enzyme, buffer and RT primer mix, samples were incubated at for 15 min at 42°C and for 3 min at 95°C. Samples were subsequently stored at -20°C until further use.

### Quantitative real-time polymerase chain reaction

Quantitative real-time polymerase chain reaction (qPCR) was done with the 7300 Real Time PCR System (Applied Biosystems). The amount of cDNA used per reaction was based on an input of 4 to 6 ng original RNA in a final volume of 20  $\mu$ l. Per reaction, 10  $\mu$ l SYBRgreen PCR Master Mix (Applied Biosystems), and 2  $\mu$ l primermix (2 pmol/ $\mu$ l) was added. Expression of selected genes was normalized to references genes 18S and GAPDH; efficiencies (E) of primerpairs were determined using LinRegPCR software. Absolute expression was calculated as:  $E^{-CT_{\text{target gene}}} / E^{-CT_{\text{reference gene}}}$ .

An overview of the forward and reverse primers used for qPCR is present in the supplementary table 1. Primers were intron-spanning, except those for CCL18 and CCR7, and were designed with the primerS in-house software package for qPCR primer design.<sup>132</sup> Sequences of all forward and reverse primers were blasted with NCBI primer-BLAST (blast.ncbi.nlm.nih.gov). Specificity of primers was further verified by assessment of dissociation curves and size fractionation on an 8% SDS-PAGE gel.

### Statistical analysis

Statistical analysis was performed with GraphPad Prism software (version 5). Mann-Whitney U tests were performed to compare CD45 and CD11b geoMFI values

between WM microglia from control donors with and without peripheral inflammation. Differences of CD45 and CD11b geoMFI values between WM and GM microglia were done using a Wilcoxon signed rank test. The same test was used to compare mRNA expression levels between unstimulated microglia and microglia cultured with mediators of either M1 or M2 activation. A p-value <0.05 was considered statistically significant.

## RESULTS

### **Intermediate CD45 expression distinguishes microglia from macrophages**

Brain tissue was collected with short post-mortem delay from 24 donors of the Netherlands Brain Bank. To phenotype cells directly *ex vivo*, flow cytometric analysis was performed on cell suspensions obtained after density gradient separation. All isolates from post-mortem brain tissue contained a population of highly autofluorescent events, a well-known phenomenon in human CNS tissue that has been ascribed to age-related accumulation of lipofuscin (data not shown).<sup>204,205</sup> Nevertheless, myeloid cells could be well discriminated from other cell types by CD11b expression. Both WM and GM contained a single CD11b<sup>+</sup> myeloid population that was further characterized as microglia, as it clearly displayed intermediate levels of CD45 expression and lower signals on forward and side scatter when compared to macrophages from choroid plexus (figure 1A – no inflammation; supplementary figure 1). At the same time, there was some overlap between WM microglia and choroid plexus macrophages for expression of CD45 and scatter characteristics (figure 1D – no inflammation). Interestingly, CD45 expression levels were constitutively lower on GM microglia compared to autologous WM microglia, whereas no significant differences were found for CD11b (figure 1B). Complete gating strategies for flow cytometric identification of microglia and choroid plexus macrophages are shown in supplementary figure 1.

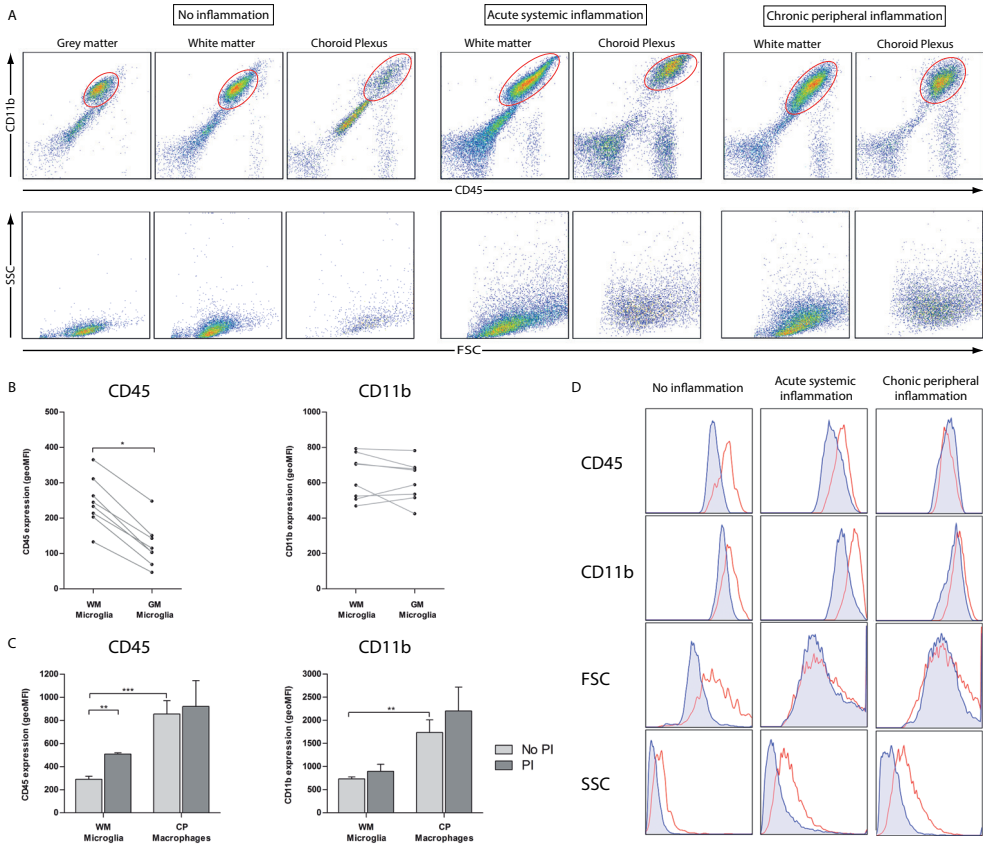


**Figure 1 Distinct phenotypes of microglia and choroid plexus macrophages and phenotypic changes of microglia associated with peripheral inflammation. (A)** Phenotypes of human microglia and choroid plexus macrophages, encircled in red, as indicated by ex vivo flow cytometric analysis for CD11b and CD45 expression in a donor without peripheral inflammation (donor 10, Table 1), a donor with sepsis (donor 9) and a donor with severe chronic wound infection (donor 11). The lower row depicts forward and side scatter of encircled populations in the upper panels, showing morphological characteristics of microglia and choroid plexus macrophages in inflammatory and non-inflammatory conditions. **(B)** Comparison of quantified expression indicates that CD45 levels are lower on GM microglia compared to autologous WM microglia, whereas CD11b expression is comparable. Data were obtained from donor 8, 10, 13, 16, 17 and 20 to 22. **(C)** Quantified expression shows that levels of CD45, but not CD11b, are significantly elevated on WM microglia isolated from donors with peripheral inflammation compared to those without peripheral inflammation (donors without peripheral inflammation:  $n=10$  for WM microglia and  $n=6$  for CP macrophages; donors with peripheral inflammation:  $n=3$  for WM microglia and  $n=3$  for CP macrophages). Data shown represent mean  $\pm$  SEM and were obtained from donor 2, 3, 9 to 11, 12 to 15, 17 to 19 and 20 (see Table 1). \* $p<0.05$ , \*\* $p<0.01$  and \*\*\* $p<0.001$ . **(D)** Histogram overlays of WM microglia (shaded histograms) and choroid plexus macrophages (open histograms) shown in panel A, indicating the various degrees of overlap for the studied parameters in diverse types of peripheral inflammation. Note the almost complete overlap for CD11b, CD45 and FSC, but not SSC, between WM microglia and autologous choroid plexus macrophages in the donor with chronic peripheral inflammation. FSC=forward scatter; SSC=side scatter; WM=white matter; GM=grey matter; CP=choroid plexus; geoMFI=geomean fluorescence intensity; PI=peripheral inflammation

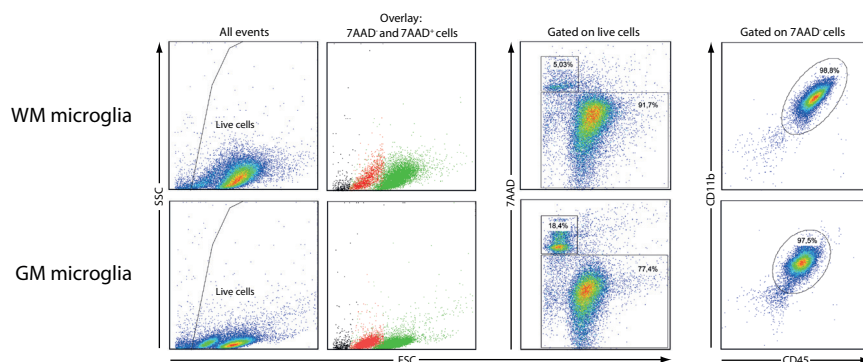


**Figure 2 Efficient isolation of primary human microglia from white and grey matter by selection with magnetic microbeads coupled to an antibody for CD11b.** Flow cytometric analysis shows that phenotypic differences between WM and GM microglia are preserved and indicates the presence of apoptotic cells that are 7AAD<sup>+</sup> (black in overlay) and a 7AAD<sup>-</sup> viable population (grey in overlay) of highly pure primary human microglia. Data were obtained from donor 13 (see Table 1). WM=white matter; GM=grey matter; FSC=forward scatter, SSC=side scatter

### Increased CD45 expression and altered morphology of microglia in peripheral inflammation

As the phenotypic markers used to define microglia might be affected by immune activation, we studied microglia phenotypes in relation to peripheral inflammatory conditions. We found that WM microglia isolated from donors with peripheral inflammation immediately prior to death displayed levels of CD45 expression that largely overlap with those of autologous choroid plexus macrophages. Moreover, these alterations went along with an increase in size and granularity, without fully abrogating the distinction with choroid plexus macrophages (figure 1A and D). Quantification revealed that WM microglia, and not choroid plexus macrophages, from donors with peripheral inflammation had significantly higher geoMFI values for CD45, but not for CD11b, when compared to those from control donors without inflammation (figure 1C). Moreover, CD45 geoMFI values correlated with both forward scatter ( $r=0.499$ ,  $p=0.021$ ) and side scatter ( $r=0.646$ ,  $p=0.002$ ), whereas CD11b geoMFI values did not (forward scatter:  $r=0.264$ ,  $p=0.248$ ; side scatter:  $r=0.224$ ,  $p=0.330$ ). This indicates that the morphological differentiation of WM microglia during immune activation specifically coincides with a strong upregulation of CD45.

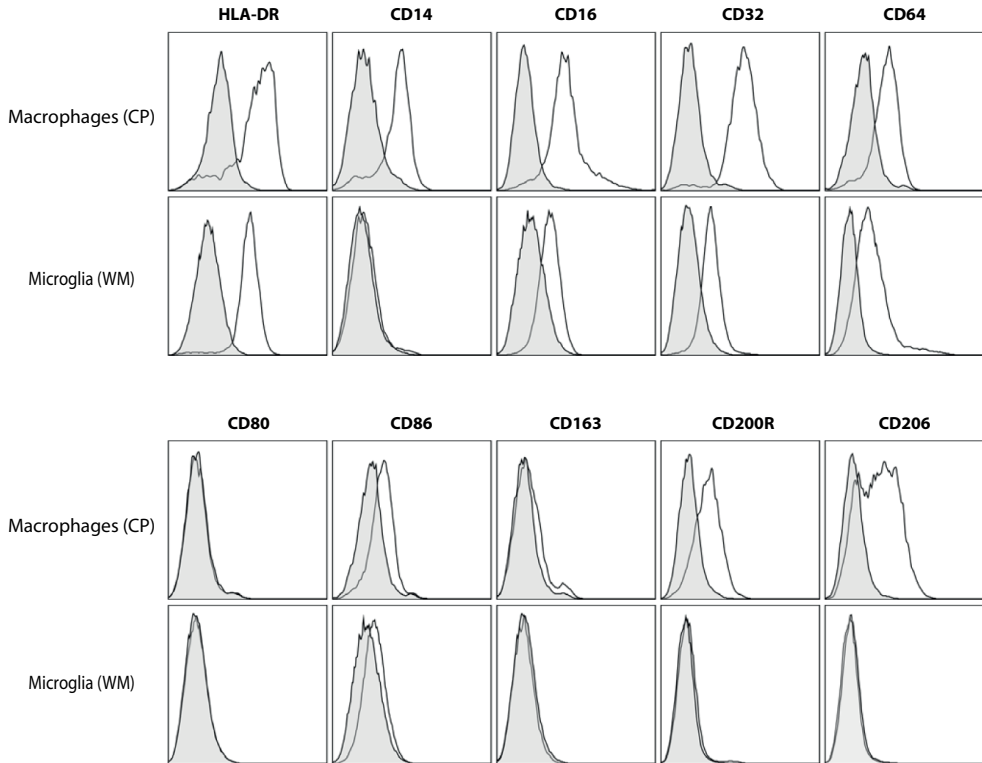


**Figure 3** Flow cytometric analysis of choroid plexus macrophages and white matter microglia *ex vivo*. Open histograms indicate stainings with the specified antibodies and shaded histograms represent stainings with appropriate isotype control antibodies. Note the clear expression of CD14, CD200R and MR (CD206) on choroid plexus macrophages, in contrast to the virtually absent expression of these molecules on the cell surface of microglia. Data were obtained from donor 23 (see table 1). CP=choroid plexus; WM=white matter

### Highly pure primary cultures of microglia obtained after selection with magnetic beads

Since cell suspensions from GM and WM after density gradient separation contained a single CD11b<sup>+</sup> myeloid population that represented microglia, we decided to sort these cells using magnetic beads coupled to an antibody for CD11b. Purity and viability of cells after MACS isolation was assessed by flow cytometry. Cell suspensions after MACS isolation contained minor populations of non-viable microglia that were 7AAD<sup>+</sup> and could be easily distinguished from the 7AAD<sup>-</sup> population of viable

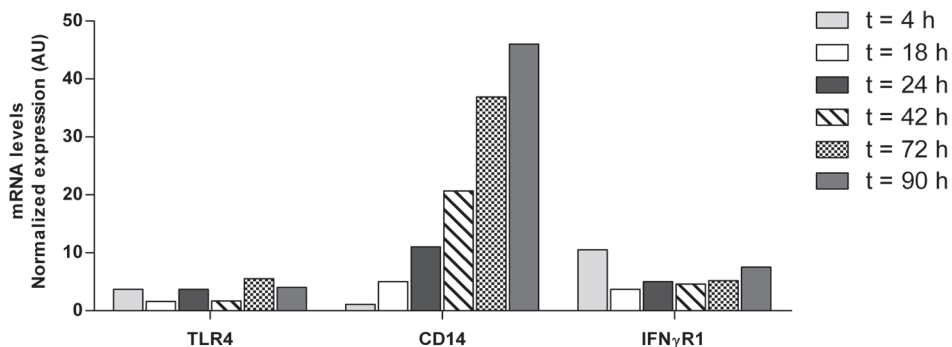


**Figure 4 Human microglia cultured under basal conditions upregulate CD14 over time.** Gene expression, as determined by qPCR analysis, in WM microglia of receptors involved in responses to LPS and IFN $\gamma$  under basal culture conditions. Note the specific upregulation of CD14, and not TLR4 and IFN $\gamma$ R1, over time. Data shown represent normalized gene expression and were obtained from donor 24 (see table 1). AU=arbitrary units

microglia by a decreased forward scatter (figure 2, overlay). Cells isolated from GM consistently contained higher percentages of 7AAD<sup>+</sup> non-viable populations, when compared to cells from WM tissue. This was also observed after density gradient separation, indicating that cell viability is not affected by the isolation procedure itself (data not shown). Thus, cortical GM cells seem to be more vulnerable to cell death, possibly due to intrinsic properties of GM microglia or as a result of differential vulnerability of cortical and callosal tissue to post-mortem delay. The large majority of cells in GM and WM isolates was 7AAD<sup>-</sup> and comprised highly enriched and viable populations of microglia, with purities of at least 97% and often more than 99% (figure 2, upper and lower right panels). Per gram of WM or GM tissue, yields of microglia varied from 50,000 to 400,000 cells. Cell yield or viability was not correlated to age, post-mortem delay or pH value of cerebrospinal fluid. In summary, the procedure allowed for rapid isolation of human microglia from post-mortem GM and WM brain tissue with high purity and yield. As corpus callosum yielded cells in most consistent and adequate numbers, subsequent experiments were performed on WM microglia.

**Microglial display a cell surface phenotype distinct from macrophages**

To more specifically establish the microglial phenotype of isolated cells, we performed flow cytometric analysis on MACS sorted WM microglia in parallel to choroid plexus macrophages. Cell surface expression of HLA-DR, CD14, CD16, CD32, CD64, CD80, CD86, CD163, CD200 receptor (CD200R) and MR (CD206) was analyzed. In strong contrast to choroid plexus macrophages, WM microglia displayed only marginal levels of CD14 and CD200R, and were completely negative for MR. In addition, expression of CD163 was totally absent on WM microglia and was hardly detected on choroid plexus macrophages. On the other hand, WM microglia did express the Fc $\gamma$  receptors CD16, CD32 and CD64, but at clearly lower levels than choroid plexus macrophages. In addition, WM microglia, like choroid plexus macrophages, markedly expressed HLA-DR, were weakly positive for CD86 and negative for CD80. All data are shown in figure 3, where histograms indicate expression detected on microglia and choroid plexus macrophages as identified by a 7AAD<sup>-</sup>CD15<sup>-</sup>CD11b<sup>+</sup>CD45<sup>dim/high</sup> phenotype using gates shown in supplementary figure 1.

**Tightly regulated M1 and distinct M2 responses of microglia *ex vivo***

Finally, we investigated whether primary microglia would show features of M1 and M2 activation when cultured with LPS and IFN $\gamma$ , IL-4 or dexamethasone. Expression of CD14 at the microglial surface was hardly detectable *ex vivo*. However, it has been reported that cultured human microglia upregulate CD14, which is crucially involved in M1 responses because of its high binding affinity for LPS.<sup>206</sup> Indeed, we observed that mRNA levels of CD14 progressively increased over time in cultured WM microglia, whereas levels of TLR4 and IFN $\gamma$ R1 did not. Therefore, we incubated cells with LPS and IFN $\gamma$  immediately *ex vivo* and harvested the following morning. We reasoned that these conditions would rule out culture effects as much as possible and more accurately reflect microglial responses *in vivo*.

Cultured WM microglia adhered to the bottom within 24 h and could be cultured for 72 h and longer (figure 5A, upper panels). Culture for 18 h in the presence of LPS alone, or in combination with IFN $\gamma$ , did not affect morphology, whereas the addition of IL-4 or dexamethasone induced specific morphological changes after

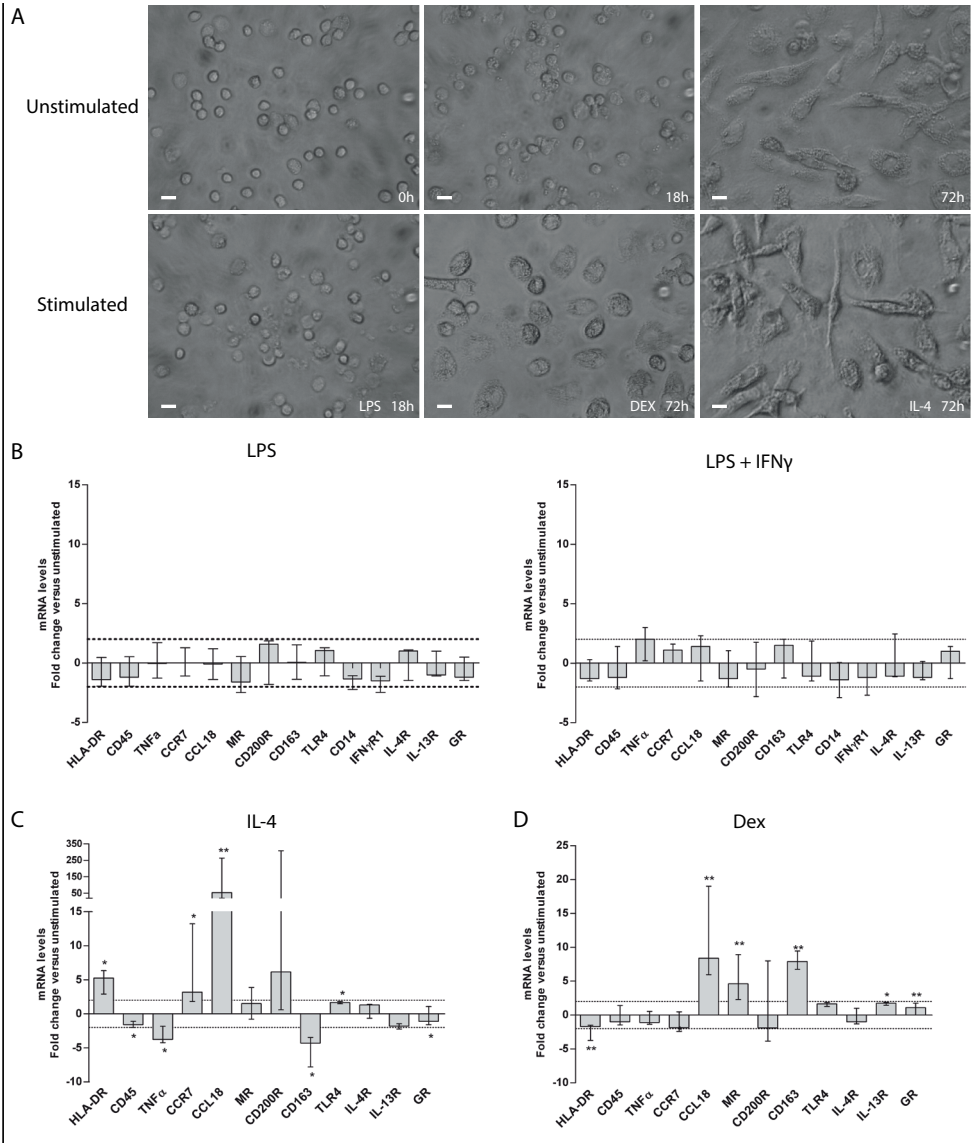


**Figure 5 Completely absent M1 responses to LPS and IFN $\gamma$  and distinct M2 responses to IL-4 and dexamethasone of primary human microglia. (A)** Morphology of WM microglia in culture directly after isolation, after 18 h and 72 h in medium only (upper row) and after 18 h with LPS and 72 h with dexamethasone or IL-4 (lower row). Scale bars represent 10  $\mu$ m. **(B)** Gene expression, as determined by qPCR analysis, in microglia after culture for 18 h with LPS, alone or in combination with IFN $\gamma$  (n=7 and n=5, respectively). **(C)** Gene expression in microglia after culture with IL-4 (n=7). Note the absence of MR and CD200R upregulation. **(D)** Gene expression after culture with dexamethasone (n=8). Note the marked upregulation of CCL18 and MR. Depicted are fold changes in mRNA levels after stimulation compared to those under basal culture conditions. Dotted lines indicate a two-fold change. Data shown represent median and interquartile range and were obtained from donor 1, 3 to 7, 10, 12 to 14, 23 and 24 (see table 1). \*p<0.05 and \*\*p<0.01. Dex=dexamethasone; GR=glucocorticoid receptor

72 h (figure 5A, lower panels). Interestingly, a complete lack of responsiveness to culture for 18 h with LPS and IFN $\gamma$  was seen in primary human WM microglia, as induction of TNF $\alpha$  and CCR7 mRNA was absent (figure 5B). In sharp contrast, human MDMs stimulated under the same conditions displayed a marked induction of TNF $\alpha$  and CCR7 (Supplementary figure 2A). Since upregulation of these molecules is known to occur fast during M1 responses in macrophages, we also cultured primary WM microglia with LPS for a shorter (4 h) time. Again, we found only a very limited M1 response in WM microglia, showing a mere 5-fold TNF $\alpha$  and 2-fold CCR7 induction, when compared to MDMs that displayed respectively a 100- and 200-fold upregulation for these genes under the same conditions (data not shown).

To verify whether M1 responsiveness would indeed be affected by culture conditions, allowing upregulation of CD14, we also stimulated WM microglia from one donor for 4 h and 18 h with LPS alone, or in combination with IFN $\gamma$ , before and after overnight culture in medium only. Clearly, overnight culture markedly augmented responses to stimulation with LPS and IFN $\gamma$  in WM microglia, as indicated by a strong upregulation of TNF $\alpha$  at the 4 h and 18 h time point and also of CCR7 after 4 h stimulation, showing that specific upregulation of CD14 in culture coincides with enhanced microglial M1 responsiveness (supplementary figure 3A and B).

In contrast to M1 stimuli, WM microglia showed evident responses to M2 stimuli. Culture with IL-4 caused an upregulation by more than a 100-fold on average of CCL18, a chemokine that is associated with M2a activation in macrophages.<sup>207</sup> HLA-DR was induced by IL-4 as well as CD200R, although the latter not significantly. Remarkably, MR was not significantly induced by IL-4, which is in strong contrast to MDMs (figure 5C and supplementary figure 2B). Culture with dexamethasone significantly upregulated CD163, MR and CCL18, the latter up to a 27-fold, in WM microglia, while induction in MDMs was mostly restricted to the classical M2c marker CD163 (figure 5D and supplementary figure 2C). Cultured GM microglia showed gene expression profiles that were highly similar to those of WM microglia in response to IL-4 and dexamethasone (data not shown).

## DISCUSSION

We here describe a procedure to rapidly isolate and culture pure microglia with high yield from post-mortem human GM and WM brain tissue of donors with and without inflammatory conditions. To our knowledge, we are the first to demonstrate phenotypic changes associated with peripheral inflammation in isolated human microglia immediately *ex vivo*. Moreover, our study demonstrates distinct responses to M2 stimuli and reveals tight regulation of M1 responsiveness in microglia.

Thus far, almost all microglia isolation procedures were time consuming as they included several enrichment steps based on differential adherent properties of glial cells types, in some cases preceded by sequential Percoll density gradient separations.<sup>115,116,208</sup> However, prolonged culture and adherence for enrichment of microglia is inevitably accompanied by changes in microglial phenotype before the start of the actual experiment. In contrast, the procedure that allows for rapid isolation of primary microglia, as described here, excludes effects of culture and adherence as much as possible. Therefore, observations made in our setup, which excludes effects of culture and adherence as much as possible, will likely more accurately reflect *in vivo* functioning of microglia. Moreover, it offers the opportunity to directly relate *ex vivo* microglial phenotypes to data obtained by downstream applications.

We obtained sufficient and viable microglia even from donors with relatively low cerebrospinal fluid pH values, whereas other reports on human microglia isolation procedures mention pH values under 7 to be associated with poor cell yield and viability. In addition, these studies do not substantiate the distinct microglial phenotype of myeloid cells isolated from brain tissue and therefore do not exclude possible contamination of isolates with blood-derived monocytes and perivascular macrophages.<sup>116,209,210</sup> In our study, CD11b<sup>+</sup>CD45<sup>high</sup> macrophages from autologous choroid plexus allowed us to verify whether myeloid cells isolated from human GM and WM displayed the specific microglial phenotype. In non-inflamed donors, a CD-11b<sup>+</sup>CD45<sup>dim</sup> profile combined with lower signals for forward and side scatter characteristics clearly differentiated microglia from choroid plexus macrophages, despite some overlap for these parameters. These findings were further corroborated by a

virtually absent expression of CD14, CD200R and MR on primary microglia, in contrast to choroid plexus macrophages, which indicated as well that any possible contamination of microglia isolates with other myeloid cell types is entirely negligible in our setup. Under conditions of peripheral inflammation, there was a clearly stronger overlap for CD45 and scatter characteristics between microglia and choroid plexus macrophages. We have preliminary data showing that under conditions of peripheral inflammation, CD11b<sup>+</sup> cells from white matter display a microglial phenotype characterized by increased but still low levels of CD14 and virtually absent expression of CD200R and MR (CD206) when compared to macrophages from choroid plexus (Melief et al., manuscript in preparation). Together, these data indicate that microglia and macrophages display, with various degrees of overlap, a continuum of CD11b and CD45 expression and scatter characteristics, but can be very well separated from each other by the use of additional markers.

Interestingly, differences in expression of CD45, but not CD11b, were present between GM and WM microglia. As low CD45 expression is associated with a more immunosuppressed state of microglia, GM microglia may be in a constitutively lower state of activation.<sup>211</sup> This would be in line with a range of studies that found expression of microglial activation markers, for example HLA-DR, to be higher in WM compared to GM in human and rat brain under both physiological and pathological conditions.<sup>212–214</sup> Moreover, region-specific differences in CD45 expression on microglia have also been reported in mouse brain.<sup>215</sup>

Quantification of CD45 protein levels revealed elevated expression on WM microglia from donors with peripheral inflammation that was correlated with increased microglial cell size and granularity. This is in line with observations that activated, or primed, microglia are characterized by an enlarged soma and stubbier ramifications, as indicated by immunohistochemical studies in mice and human.<sup>110,216,217</sup> This study is therefore the first to show microglial activation related to peripheral inflammation in isolated human microglia *ex vivo*. Several lines of research indicate that effects of systemic inflammation on the immune status of microglia may result in enhanced responsiveness to ensuing inflammatory challenges and negatively affect clinical progression of neurodegenerative diseases.<sup>110,111</sup> As such, quantification of CD45

protein levels might be used to assess microglial activation and can be related to data from *in vitro* studies on microglial immune responses. Additionally, more extensive analysis is warranted of the phenotypic changes of human microglia associated with systemic inflammation, with particular focus on regulation of molecules known to be involved in initiation or suppression of pro-inflammatory immune responses and neurotoxicity. Together, these approaches may give more insight into mechanisms of (detrimental) microglia activation and progression of neurodegenerative diseases due to inflammatory episodes.

Importantly, our approach makes it possible to directly relate *ex vivo* microglial phenotypes to observations made in functional assays for features such as immune responsiveness, phagocytosis and T-cell interactions on the one hand, and transcriptomic and proteomic analyses on the other hand. As a first step, we investigated here the cellular activation of freshly isolated microglia directly *ex vivo*. A possible explanation for the unresponsiveness of microglia to LPS and IFN $\gamma$  in culture is the virtually absent expression of CD14 at the microglial cell surface *ex vivo*. This observation is in line with other human studies reporting absent mRNA and protein levels of CD14 in resting microglia *in situ* and *ex vivo*.<sup>115,196,206,218</sup> As CD14 binds LPS with high affinity and together with TLR4 facilitates transmembrane signaling, its absent expression might underlie the initial lack of M1 responsiveness of primary human microglia towards this stimulus.<sup>219</sup> This idea is supported by the finding that a specific increase of CD14, and not TLR4 and IFN $\gamma$ R1 mRNA levels during culture of primary human microglia coincides with enhanced M1 responsiveness after incubation with LPS and IFN $\gamma$  for 4 h and 18 h. This may also explain why M1 responses were observed in a recent study of human microglia in which LPS stimulation was preceded by several days of culture in the presence of granulocyte-macrophage colony-stimulating factor.<sup>220</sup> Interestingly, human WM microglia in our hands did also not respond to IFN $\gamma$  in co-cultures with LPS, although it is well-known for its M1 inducing capabilities in human macrophages. Absent *in situ* expression of receptors for IFN $\gamma$  has been reported for human microglia, even in pathological conditions.<sup>221</sup> Together, these findings imply that resting microglia are inherently non-responsive towards M1 stimuli *in vivo*. This may represent an intrinsic property of human microglia to not be

overtly activated by pro-inflammatory stimuli in order to prevent neurotoxicity and CNS tissue damage.

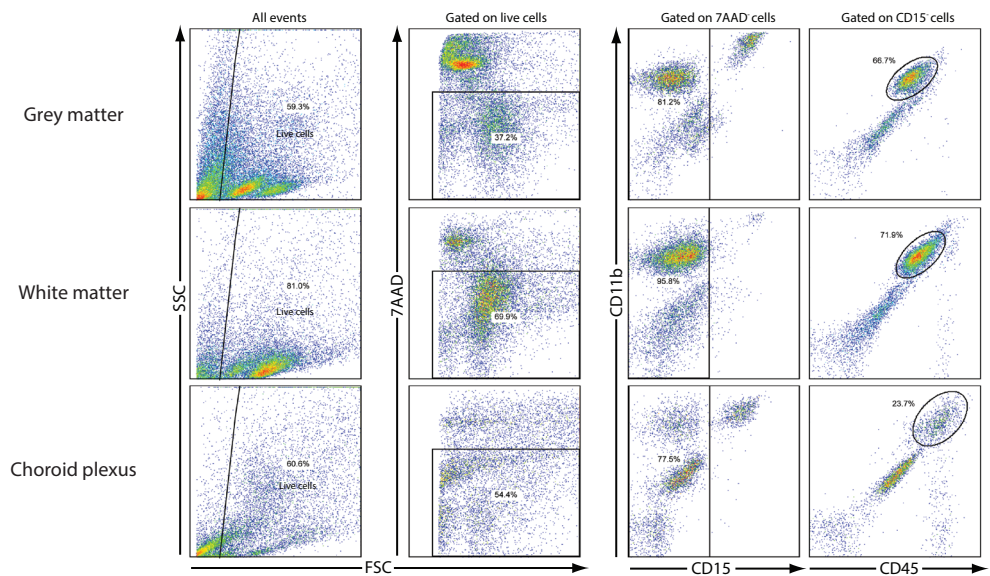
In contrast to what was observed for LPS and IFN $\gamma$ , primary human microglia were clearly responsive to M2 stimuli. Responsiveness of human microglia to IL-4 was indicated by a M2a markers, such as CCL18 and HLA-DR and, to a lesser extent, CD200R.<sup>83,84,222</sup> Conversely, we observed no induction of the MR, which is a hallmark of M2a activation of MDMs. Culture of microglia with dexamethasone caused consistent induction of CD163 and upregulated CCL18 with similar strength. CD163 is a well-established and highly specific M2c macrophage marker, which has also been found to be expressed by microglia in and around multiple sclerosis (MS) lesions.<sup>143</sup> However, marked upregulation of CCL18 by glucocorticoids has not been described for macrophages to our knowledge and it was indeed only weakly induced by dexamethasone in human MDMs in our hands.<sup>223</sup> It has been shown recently that CCL18 by itself induces in human monocytes an M2-like macrophage phenotype in absence of IL-4, resulting in production of IL-10 and an increased capacity for phagocytosis.<sup>224</sup> Overall, these data lead to the conclusion that microglia exhibit distinct features of alternative activation, as indicated by specific gene expression profiles induced by the M2 mediators dexamethasone and IL-4.

In summary, the present study demonstrates a new and robust method for rapid isolation and culture of primary human microglia from post-mortem brain tissue and offers new opportunities for fundamental studies on microglia biology. Moreover, it emphasizes the importance to perform functional assays on microglia immediately after isolation, as this excludes effects of phenotypic changes brought about by culture. Finally, our data shed new light on the phenotypic and functional properties of microglia in the human CNS, thereby contributing to future research on modulation of microglial functioning as a therapeutic intervention in neurological disorders.

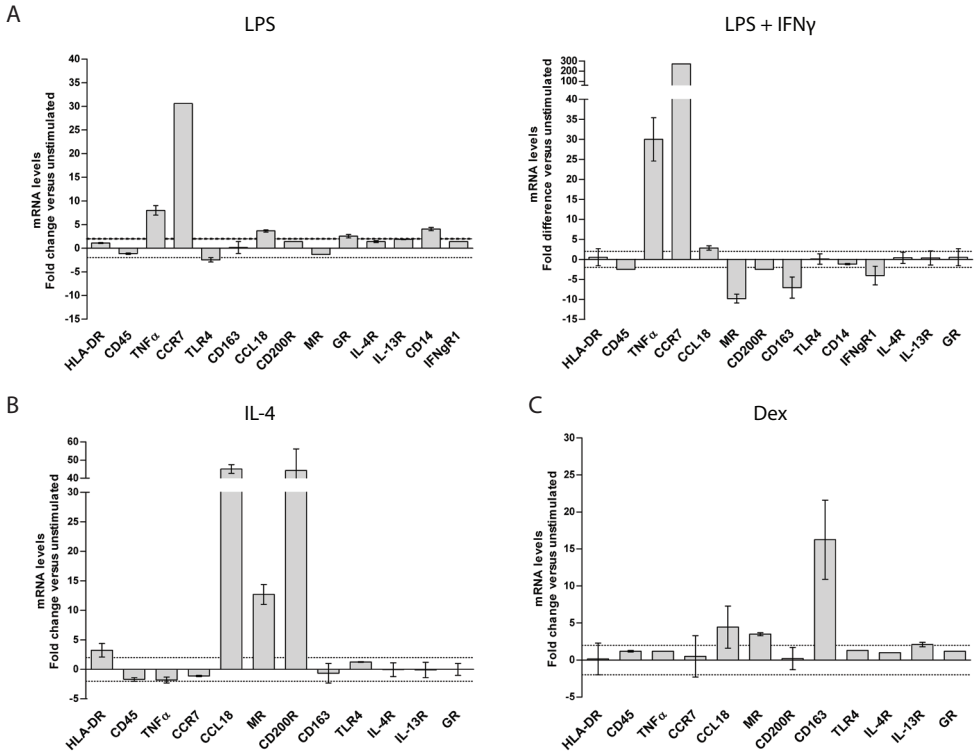
## ACKNOWLEDGEMENTS

We thank the NBB team for their excellent services ([www.brainbank.nl](http://www.brainbank.nl)). This work was supported by a grant from the Dutch Multiple Sclerosis Research Foundation (grant number MS 525\_EXT).

## SUPPLEMENTAL DATA



**Supplementary figure 1** Gating strategy for ex vivo flow cytometric phenotyping of microglia from grey matter and white matter and macrophages from choroid plexus. Data were obtained from donor 10 (see table 1). FSC=forward scatter; SSC=side scatter



**Supplementary figure 2 M1 and M2 responses of human monocyte-derived macrophages. (A)** Gene expression, as determined by qPCR analysis, after culture for 18 h with LPS alone, or in combination with IFN $\gamma$ . **(B)** Gene expression after culture for 72 h with IL-4. Note the marked upregulation of MR and CD200R. **(C)** Gene expression after culture for 72 h with dexamethasone. Note the limited upregulation of CCL18. Depicted are fold changes in mRNA levels after stimulation compared to those under basal culture conditions (n=2). Dotted lines indicate a two-fold change. Data shown represent median and interquartile range (donors not depicted in table 1). Dex=dexamethasone

**Supplementary table 1** Primer sequences used for gene expression analysis

Protein	Database no.	Primer sequence forward	Primer sequence reverse
HLA-DR	NM_019111	CCCAGGGAAGACCACCTTT	CACCTGCAGTCGTAACCGT
CD45	NM_002838.3	GCAGCTAGCAAGTGGTTTGTTCC	AAACAGCATGCGTCCTTTCTC
CD14	NM_000591.3	ACAGGGCGTTCTTGGCTCGC	CGGGAAGGCGCAACCTGTT
TNF $\alpha$	NM_000594	ATGTCCCAAGACAAGGGCAAGA	GGGCAGTCAATGGTCAGATATTGA
CCR7	NM_001838.3	TGAGGTCACGGACGATTACAT	GTAGGCCACGAAACAATGAT
CCL18	NM_0002988.2	CCCAGCTCACTCTGACCACT	GTGGAATCTGCCAGGAGGTA
MR	NM_002438	TGCAGAAGCAAACCAACTGTAA	CAGGCCTTAAGCCAACGAACT
CD200R	NM_138806	GAGCAATGGCACAGTGACTGTT	GTGGCAGGTCACGGTAGACA
CD163	NM_004244.5	AAGACGCTGCAGTGAATTGCA	GGATCCCAGTCAATAAAGGAT
TLR4	NM_138554.4	TACAAAATCCCCGACAACCTC	AGCCACCAGCTTCTGTAACT
IFN $\gamma$ R1	NM_00416.2	CGATTATGATCCCGAAACTACCTGTT	CTGAATCTCGTCACAATCATCTTCTC
IL-4R	NM_000418.2	CGCTTTCCTGCATTGTCATCCT	GGCTGGGTTGGGAATCTGAT
IL-13R	NM_001560.2	TGCTATGAGGATGACAAACTCTGGAGTA	CGACGATGACTGGAACAATGAGTAACAT
GR	NM_001018077	GGATCCCGACTGCAATAAAGGAT	CACCCGATCCACCTCACCTT